Nuclear Physics and Medical Imaging

Greg Mitchell
gsmitchell@ucdavis.edu
Department of Biomedical Engineering
UC DAVIS
UNIVERSITY OF CALIFORNIA

In Vivo Biomedical Imaging

	ultrasound
Anatomic	x-ray CT
Physiologic	MRI
Metabolic	PET/SPECT
Molecular	optical imaging

UC DAVIS UNIVERSITY OF CALIFORNIA — cmgi

Probing Tissue with Radiation

$$E = h\nu = hc/\lambda \qquad c = \lambda\nu$$

ELECTROMAGNETIC SPECTRUM

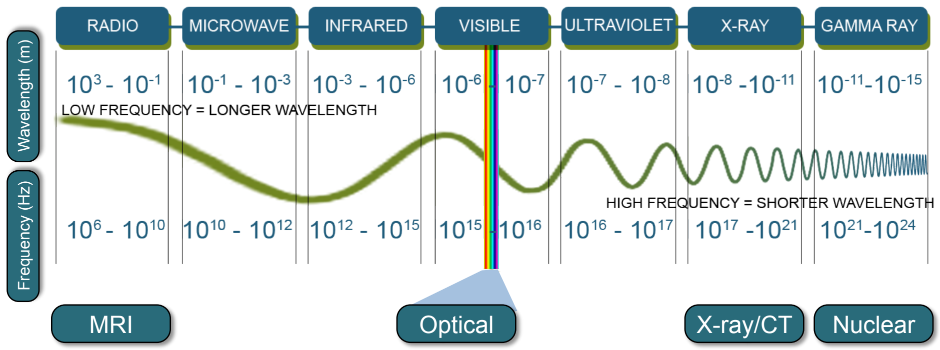

WHAT IS NUCLEAR IMAGING?

NUCLEAR IMAGING

- Imaging the distribution of radioactively tagged substances that are introduced into a living subject

- The radiolabeled agents that are injected are called
  - Radiotracers (or just tracers for short)
  - Radiopharmaceuticals
  - Probes

BRIEF HISTORY

1896: DISCOVERY OF RADIOACTIVITY
HENRI BECQUEREL - NOBEL PRIZE 1903

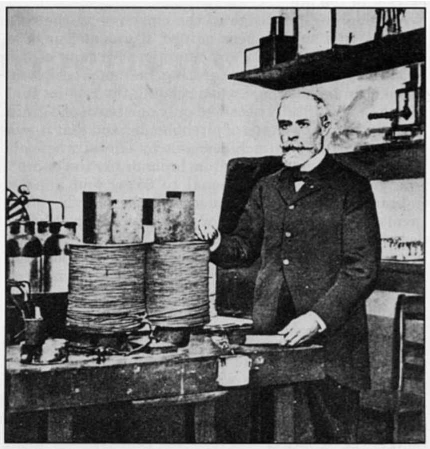

[2.1] Antoine Henri Becquerel in his laboratory. (Courtesy: Museum Marii Sklodowskiej-Curie, Warsaw.)

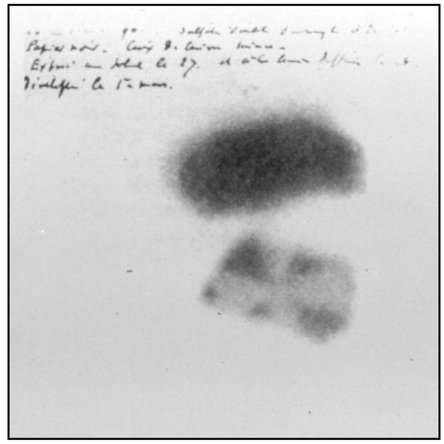

(IMAGING!)

1923: FIRST USE OF RADIOACTIVE TRACER
GEORG DE HEVESY - NOBEL PRIZE 1943

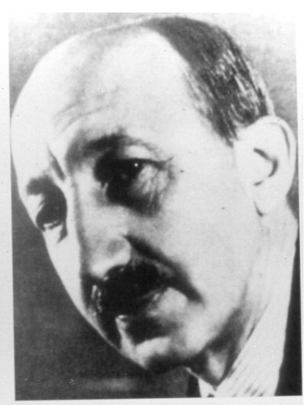

1923: ^{212}Pb to study absorption and translocation of lead nitrate in bean plants

1935: ^{32}P - first use of artificially produced radioisotopes

1942: in vitro labeling of red blood cells

1930's: DEVELOPMENT OF THE CYCLOTRON
ERNEST O. LAWRENCE - NOBEL PRIZE 1939

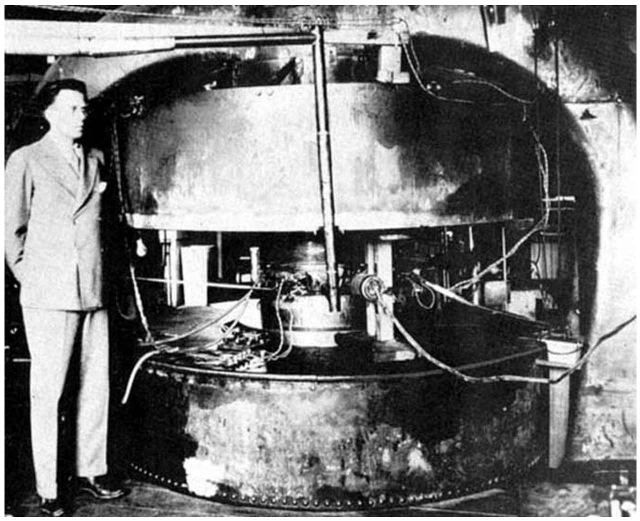

1938: DISCOVERY OF ^{99m}Tc and ^{131}I
GLENN SEABORG - NOBEL PRIZE 1951
EMILIO SEGRE - NOBEL PRIZE 1959

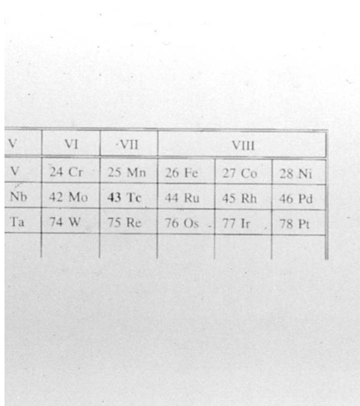

V	VI	VII	VIII		
V	24 Cr	25 Mn	26 Fe	27 Co	28 Ni
Nb	42 Mo	43 Tc	44 Ru	45 Rh	46 Pd
Ta	74 W	75 Re	76 Os	77 Ir	78 Pt

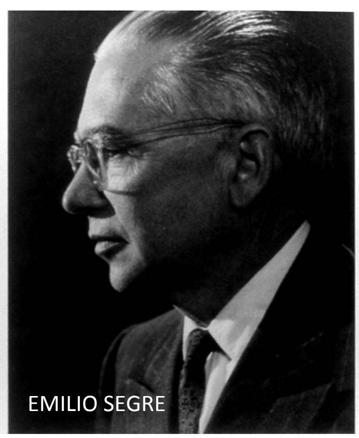

TECHNETIUM WAS FIRST ARTIFICIALLY MADE ELEMENT

1956: INVENTION OF THE GAMMA CAMERA
HAL ANGER

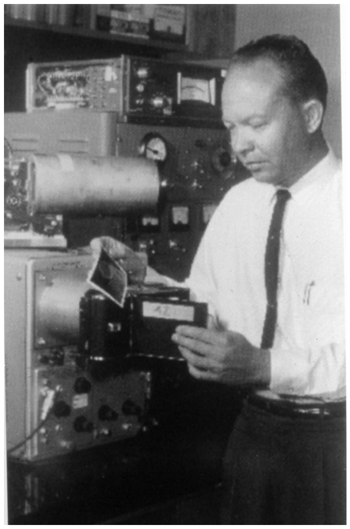

1975: FIRST PET SCANNER
MICHAEL PHELPS, EDWARD HOFFMAN
& MICHAEL TER-POGOSSIAN

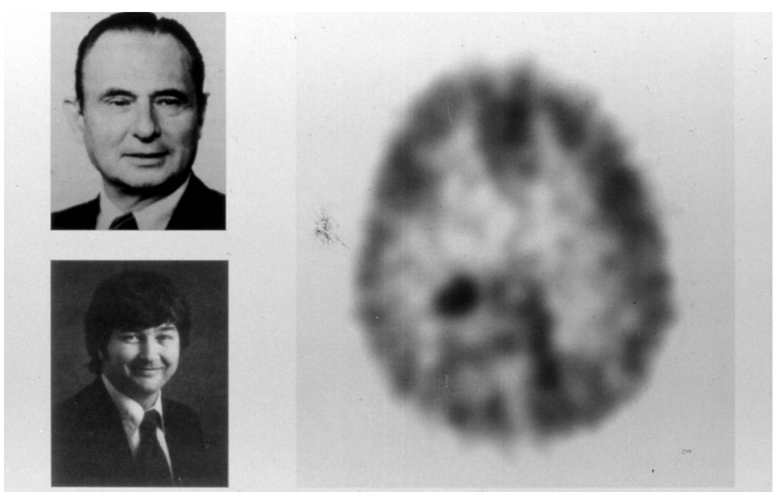

MODERN
NUCLEAR IMAGING
-- SPECT AND PET --

SINGLE PHOTON EMISSION COMPUTED TOMOGRAPHY

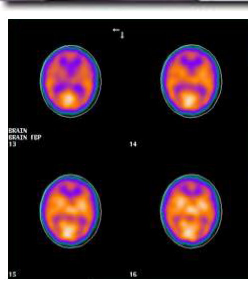

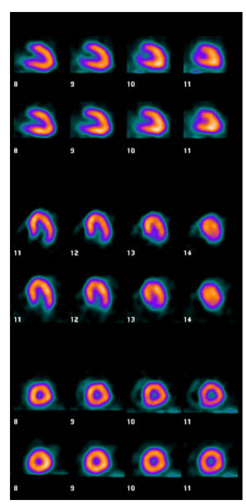

Clinical SPECT and SPECT/CT Scanners

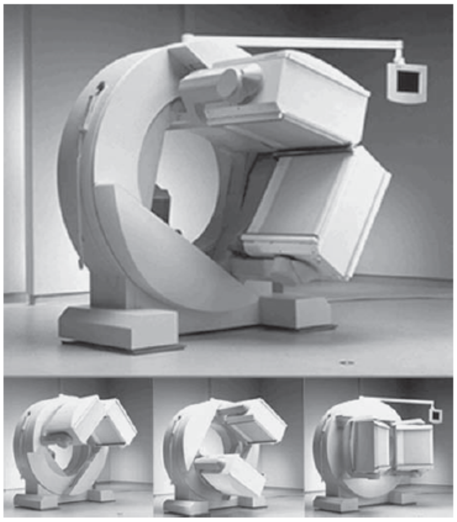

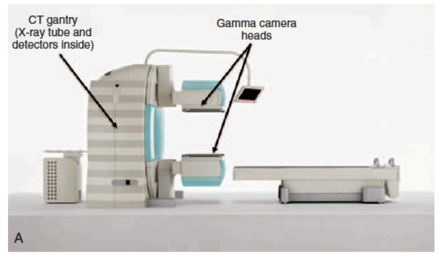

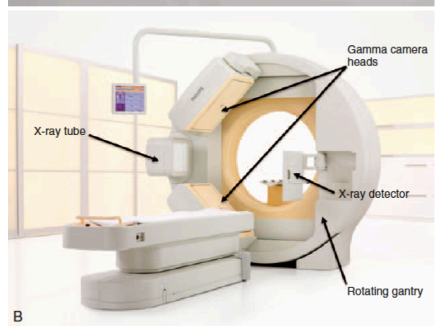

Images courtesy Siemens and Philips

Types of Collimation used in Gamma Cameras

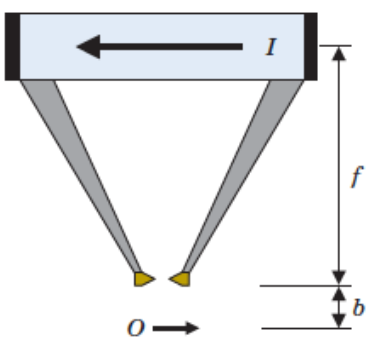

Pinhole Collimation

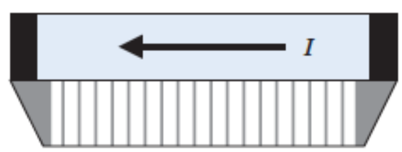

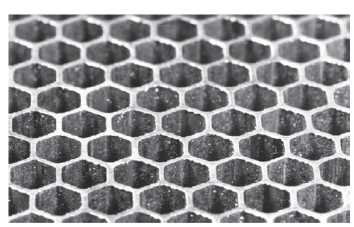

Parallel-Hole Collimation

In Vivo Imaging as a Translational Tool

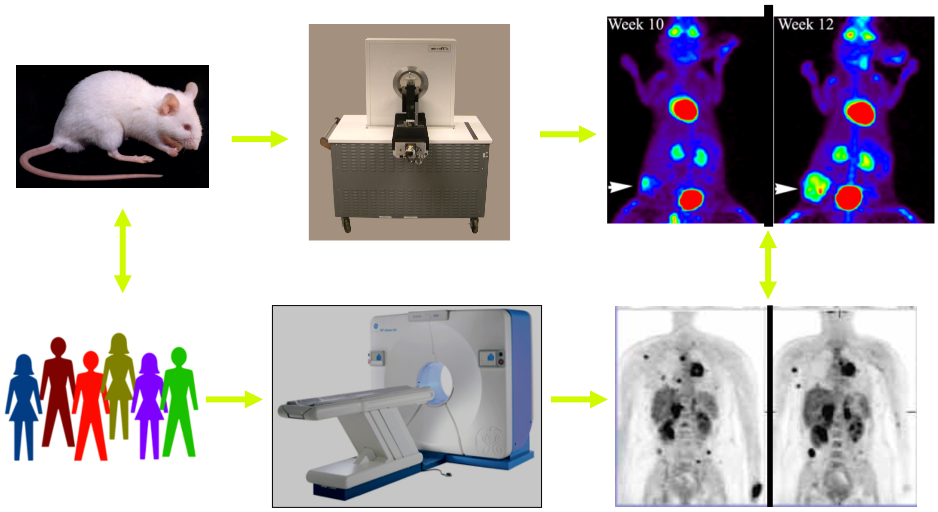

Preclinical SPECT and SPECT/ CT Scanners

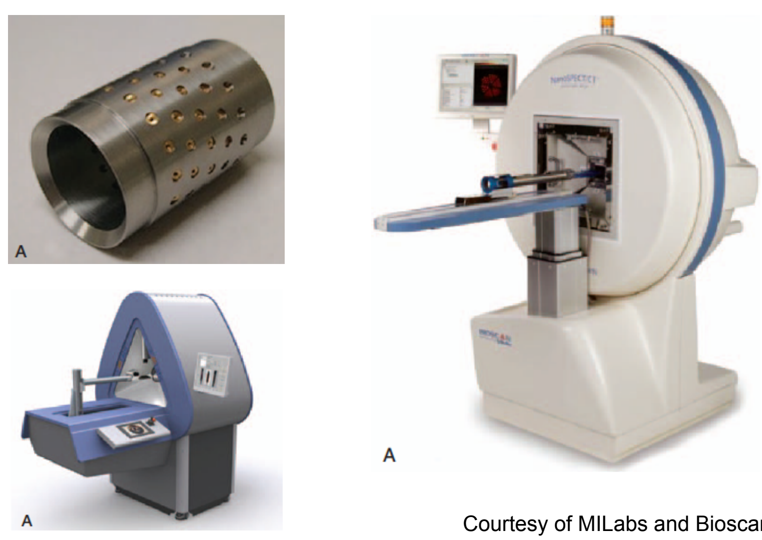

Courtesy of MILabs and Bioscan

Molecular Imaging with SPECT

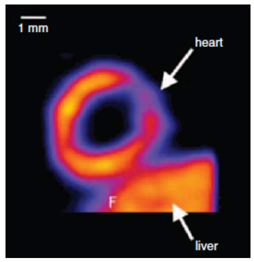

Myocardial perfusion,
^{99m}Tc-sestamibi (Bioscan)

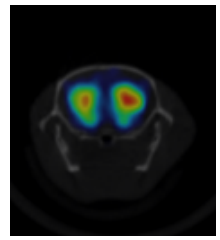

Dopamine transporter,
^{123}I-Ioflupane (MILabs)

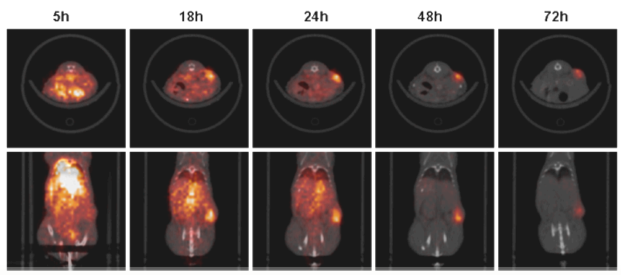

Tumor targeting, ^{125}I-telodendrimer loaded with paclitaxel (Kit Lam, UC Davis)

POSITRON EMISSION TOMOGRAPHY

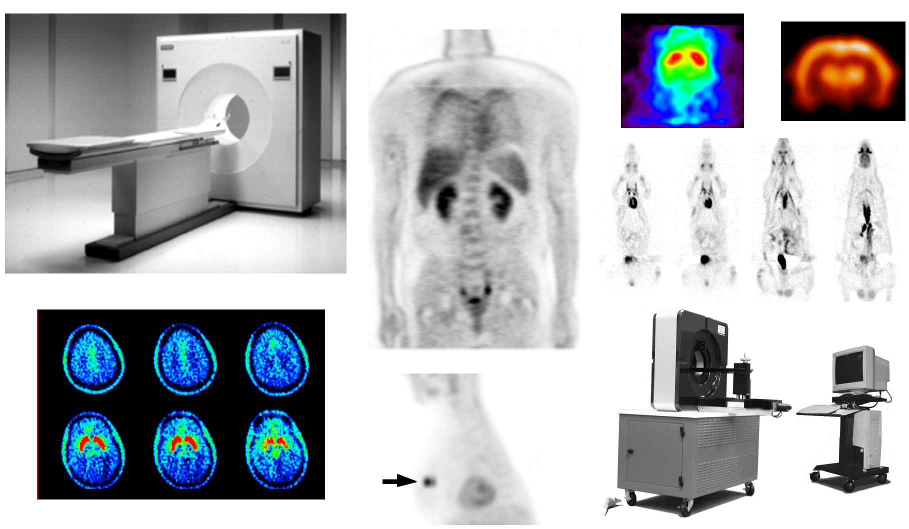

Clinical PET and PET/CT Scanners

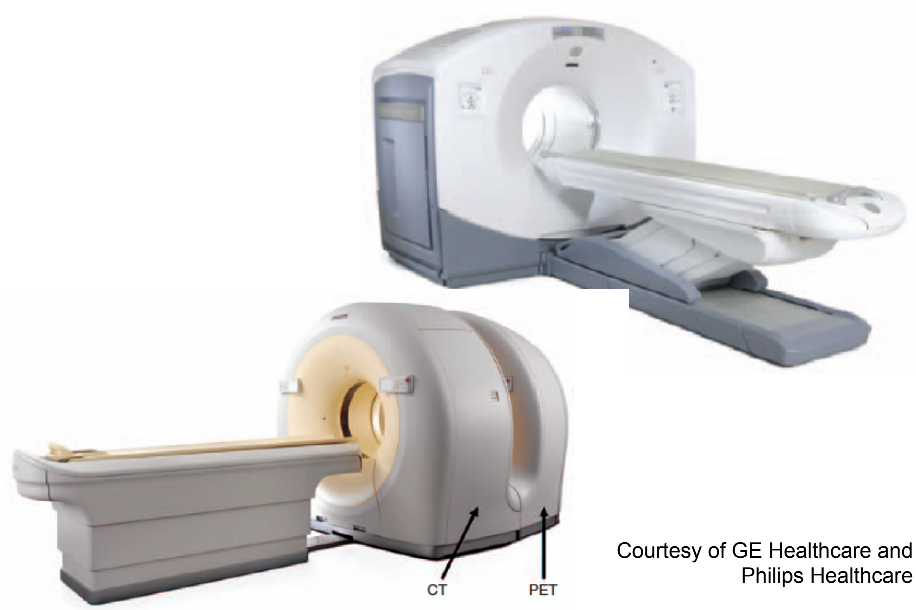

Courtesy of GE Healthcare and Philips Healthcare

What is PET?

Provides molecular or functional information of a biological system by imaging the distribution of a targeted radiotracer

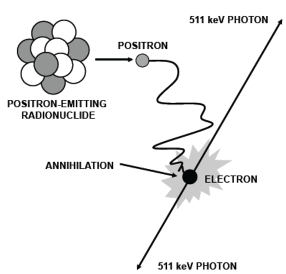

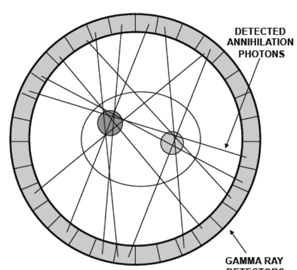

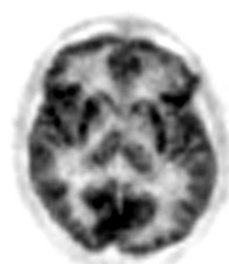

Applications
Oncology: Detection and staging in cancer
Cardiology: Myocardial viability
Neurology: Psychiatry, differentiating NGD (Alzheimer's, Parkinson's, etc.)

Figures from Cherry *et al*, Physics in Nuclear Medicine.

Angular Projections in PET

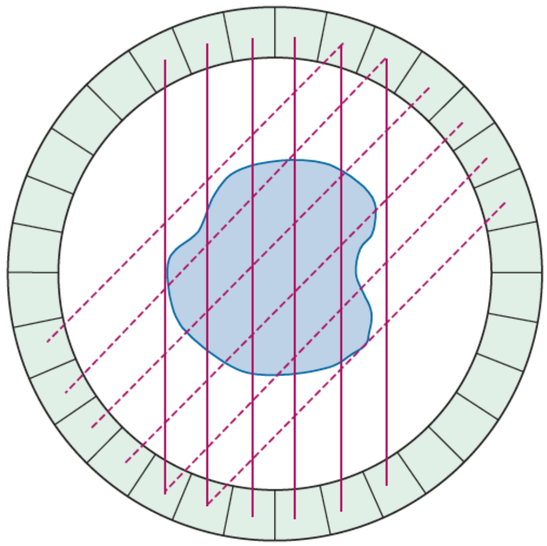

Reconstruction in PET/SPECT

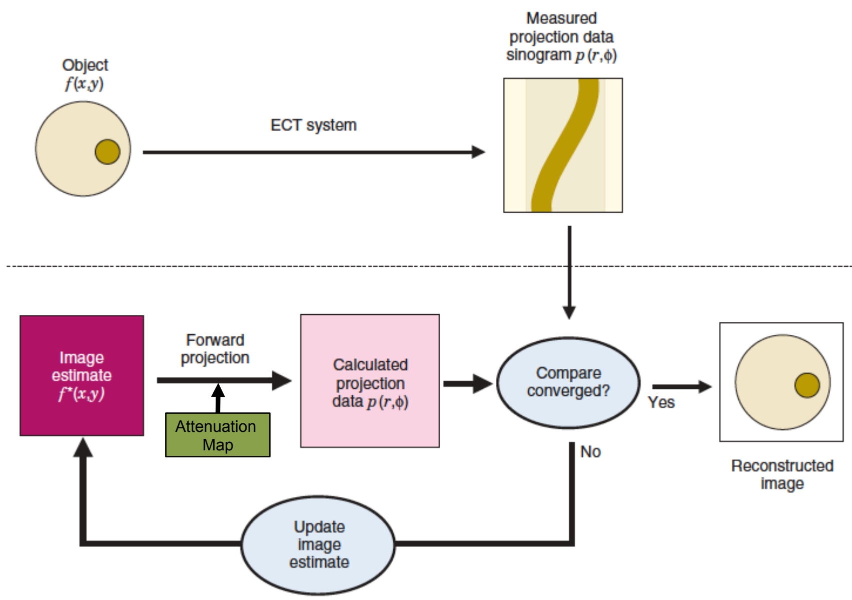

Scintillation Detector

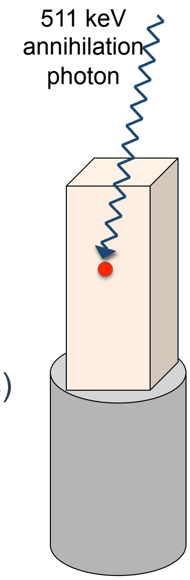

- Scintillator
  - Emits light when radiation strikes it
  - Amount of light released is proportional to amount of energy deposited
  - Amount of light released is small (10^4-10^5 photons per MeV)
  - Optically transparent (to its own emissions)
- Sensitive Photodetector
  - Converts light into an electrical signal
    - Photomultiplier Tubes (PMTs)
    - Photodiodes, Avalanche Photodiodes, SiPMs

Scintillators for PET

Property	NaI(Tl)	BGO	LSO(Ce)	GSO(Ce)	CsI(Tl)	LuAP(Ce)	$LaBr_3$(Ce)
Density (g/cm^3)	3.67	7.13	7.40	6.71	4.51	8.34	5.3
Effective atomic number	50	73	66	59	54	65	46
Decay time (nsec)	230	300	40	60	1000	18	35
Photon yield (per keV)	38	8	20-30	12-15	52	12	61
Index of refraction	1.85	2.15	1.82	1.85	1.80	1.97	1.9
Hygroscopic	Yes	No	No	No	Slightly	No	Yes
Peak emission (nm)	415	480	420	430	540	365	358

*Typical values—there are many different plastic scintillators available.
BGO, $Bi_3Ge_4O_{12}$; GSO(Ce), Gd_2SiO_5(Ce); LSO(Ce), Lu_2SiO_5(Ce); LuAP(Ce), $LuAlO_5$(Ce)

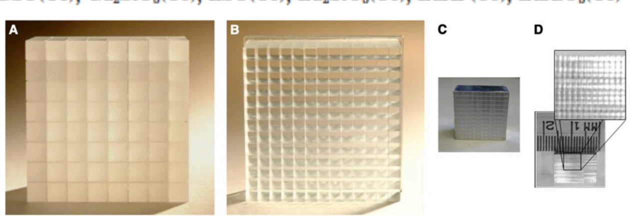

Detector Technology Used in PET

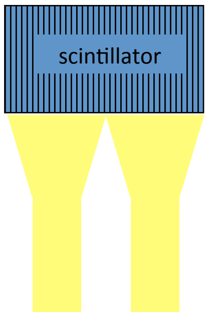

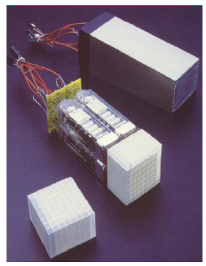

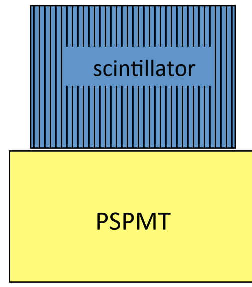

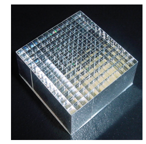

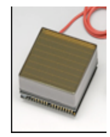

array of photomultiplier tubes

position-sensitive photomultiplier tube

PET Applications

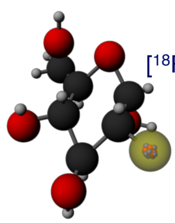

[^{18}F]-fluoro-2-deoxy-D-glucose
(FDG)

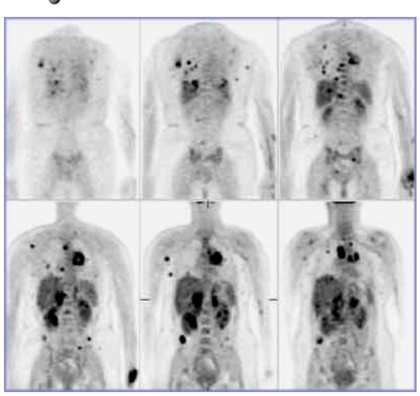

Images courtesy of GE Medical Systems

^{11}C-PIB
AMYLOID PLAQUE BURDEN

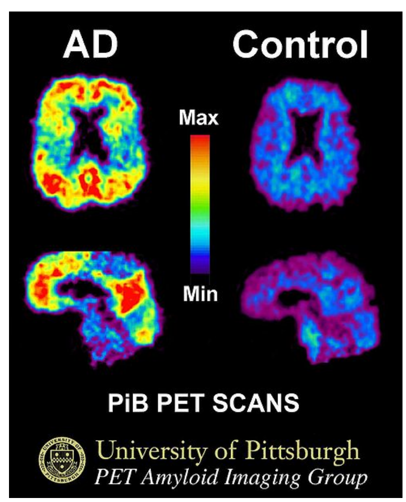

Radiotracers/Radiopharmaceuticals

- Usually introduced by i-v injection
- Agent must have access to target
  - Stable in plasma
  - For extravascular targets, passive diffusion or active transport into extracellular space
  - For targets in the brain, cross blood-brain barrier
  - For intracellular targets, must get across cell membrane
- Agent must be modified by interaction with target
  - Binding, trapping, ….
- Unmodified agent must be cleared away
  - Efficient clearance and excretion from body
- Many parallels with drug design, but some important differences as well

COMPACT BIOMEDICAL CYCLOTRON 11 MeV negative ion

^{18}F (110 mins)
^{11}C (20 mins)
^{13}N (9.9 mins)
^{15}O (120 s)

Some Examples of Radiopharmaceuticals for PET

- ^{18}F-FDG ([^{18}F]fluoro-2-deoxy-D-glucose)
  - Targets glucose transporters and hexokinase
  - Rate of glucose utilization
- ^{18}F-FLT (3'-deoxy-3'-[^{18}F]fluorothymidine)
  - Targets thymidine kinase 1
  - Proliferation (thymidine uptake and phosphorylation)
- ^{18}F-FMISO ([^{18}F]fluoromisonidazole)
  - Targets hypoxic tissue
- ^{18}F-FHBG (9-(4-[^{18}F]fluoro-3-hydroxymethylbutyl)guanine)
  - HSV-tk transgene expression
- ^{64}Cu or ^{124}I-labeled biomolecules
  - Peptides, antibdodies, nanoparticles and cells

^{99}Mo–^{99m}Tc GENERATOR

- ^{99}Mo bound to alumina column as molybdate ion (MoO_4)
- ^{99m}Tc activity is not bound to column (chemically different)
- Eluted from column with 5-25 mL saline
- 75-85% of available ^{99m}Tc extracted
- Typically used for one week

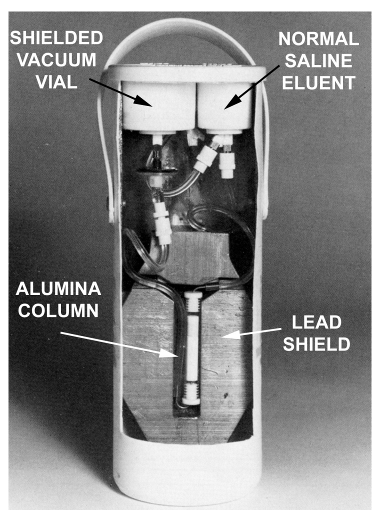

RADIONUCLIDES USED FOR IMAGING/ THERAPY

Radionuclide	Decay Mode	Principal Photon Emissions	Halflife	Primary Use
^{11}C	β^+	511 keV	20.3 min	imaging
^{13}N	β^+	511 keV	10.0 min	imaging
^{15}O	β^+	511 keV	2.07 min	imaging
^{18}F	β^+	511 keV	110 min	imaging
^{32}P	β^-	–	14.3 days	therapy
^{67}Ga	EC	93, 185, 300 keV	3.26 days	imaging
^{82}Rb	β^+	511 keV	1.25 min	imaging
^{89}Sr	β^-	–	50.5 days	therapy
^{99m}Tc	IT	140 keV	6.03 hours	imaging
^{111}In	EC	172, 247 keV	2.81 days	imaging
^{125}I	EC	27-30 keV x-rays	60.2 days	in vitro assays
^{123}I	EC	159 keV	13.0 hours	imaging
^{131}I	β^-	364 keV	8.06 days	therapy/imaging
^{153}Sm	β^-	41, 103 keV	46.7 hours	therapy
^{186}Re	β^-	137 keV	3.8 days	therapy
^{201}Tl	EC	68-80 keV x-rays	3.05 days	imaging

[END OF HISTORY & SURVEY]

Aside on speaker's background...

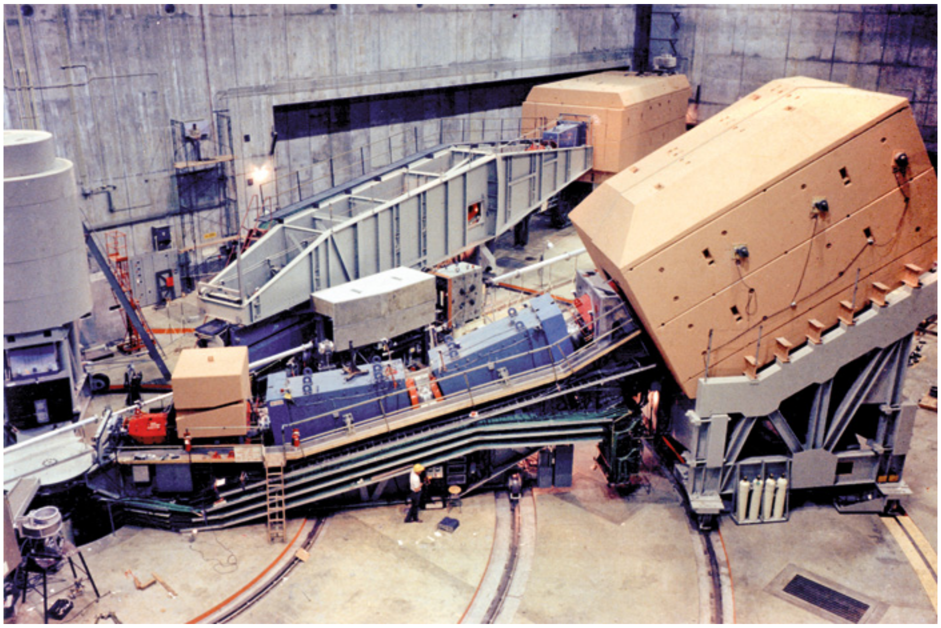

SLAC E154/E155/E155X

(Late 1990's at SLAC)

Polarized inclusive DIS to measure spin structure functions

$$g_1 = \frac{F_1(x,Q^2)}{D'}(A_{\parallel} + \tan(\theta/2)A_{\perp})$$

$$g_2 = \frac{F_1(x,Q^2)}{D'}\frac{y}{2\sin\theta}(\frac{E+E'\cos(\theta)}{E'}A_{\perp} - \sin(\theta)A_{\parallel})$$

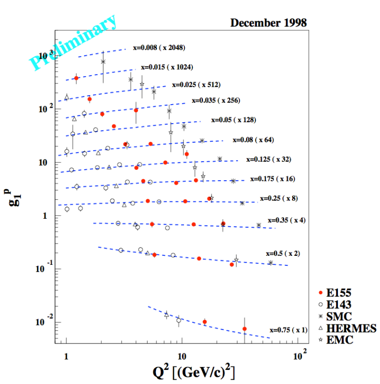

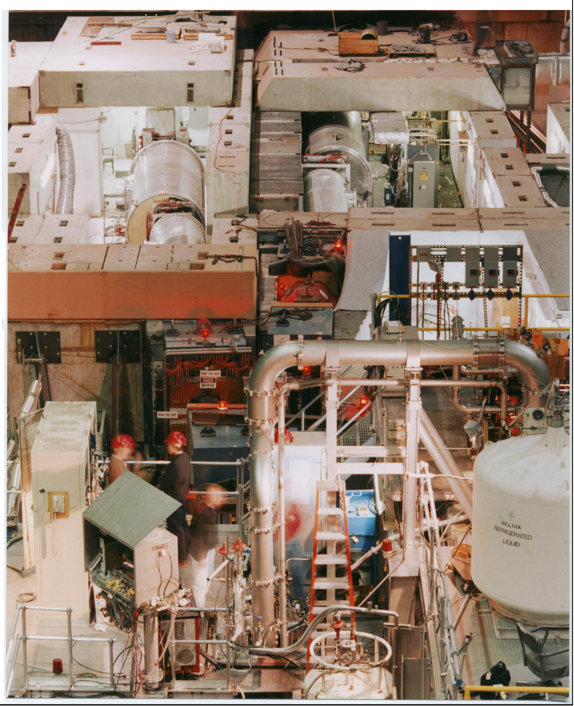

Los Alamos
NATIONAL LABORATORY
EST.1943

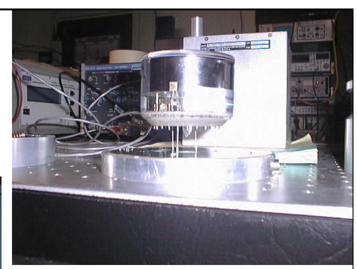

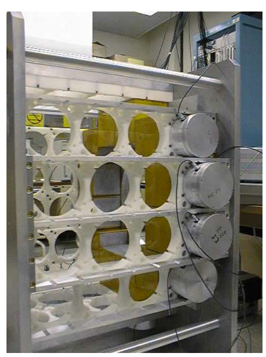

$$\vec{n} + p \rightarrow d + \gamma$$

The NPDGamma Experiment (LANSCE at LANL and FNPB at SNS)

Polarized cold neutron capture on LH_2 target

ppb up-down asymmetry → Parity violation to study the hadronic weak interaction

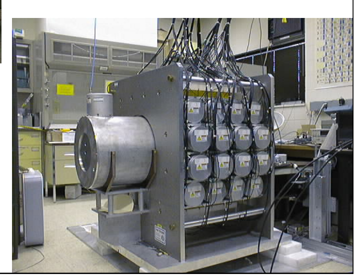

JLab E02-020

Measure the parity-violating asymmetry in e-p elastic scattering at $Q^2 = 0.03\ GeV^2$ to 4% relative accuracy

Extract the proton weak charge and thus the weak mixing angle at low momentum transfer

$$Q^p_{weak} = 1 - 4\sin^2\theta_W \sim 0.072$$

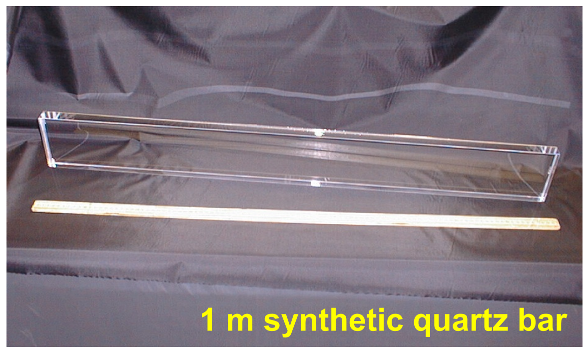

PET AND SPECT SYSTEMS ARE NUCLEAR PHYSICS EXPERIMENTS

Photodetectors at UC Davis

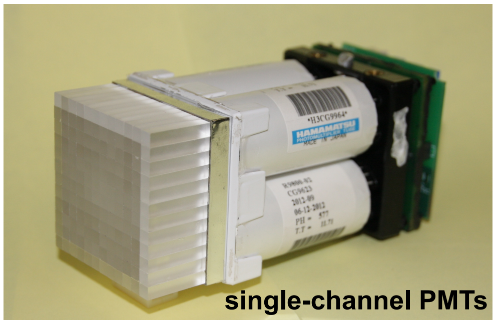

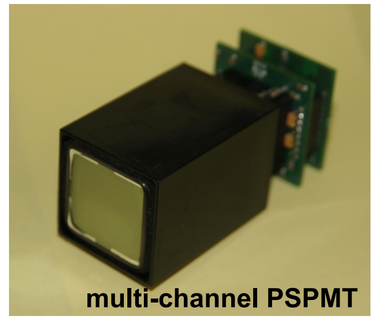

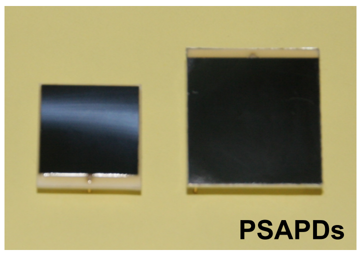

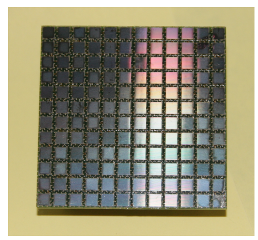

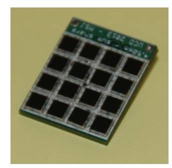

SiPMs

Some specific research projects at UC Davis

New detector materials: Thallium Bromide (TlBr)

Gamma ray detectors for PET

- Efficiency & energy resolution

Table 1. Properties of Detector Materials Used for PET

	LSO	**$LaBr_3$**	**BGO**	**CZT**	**TlBr**
Detector type	Indirect	Indirect	Indirect	Direct	**Direct**
Z_{eff}	66	47	75	50	**80**
Density (g/cc)	7.4	5.1	7.1	6	**7.56**
Photofraction, 511 keV (%)	34	15	41	17	**42**
Attenuation Length, 511 keV (cm)	1.2	2.1	1.1	1.8	**1.05**
Number of photons (or e-h pairs) per 1 MeV γ-ray Energy	24,000 photons	63,000 photons	8,200 photons	$2x10^5$ e-h pairs	**$1.5x10^5$ e-h pairs**

RMD grown crystals

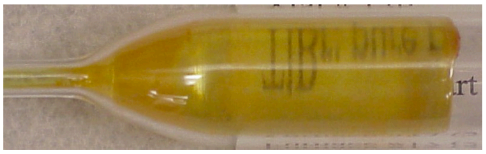

Figure 11. Photograph of a 1.6 cm diameter TlBr ingot with >3 cm length grown by vertical Bridgman method.

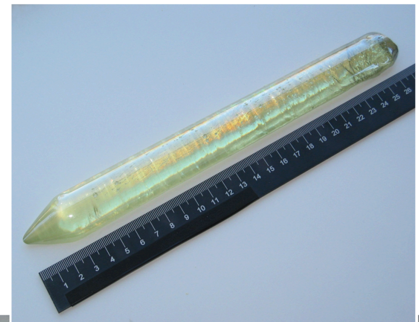

Figure 6. TlBr ingot, purified and grown with traveling molten zone method, 30-mm diameter by 270-mm long.

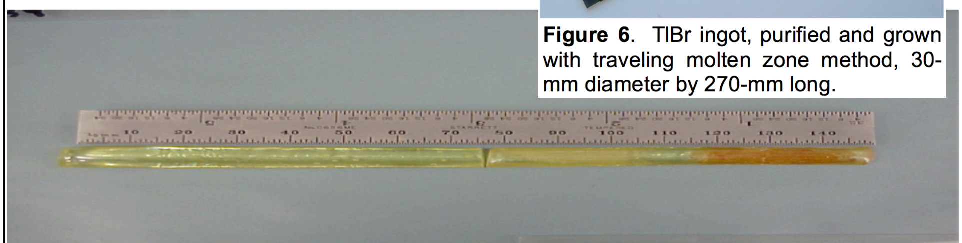

Figure 9. Photograph of a TlBr ingot taken out from the quartz ampoule. This ingot was zone refined (30 +1 passes) under an atmosphere of ~ 250-mm Hg of HBr. The last pass was ten times slower than the 30 zone refining passes to allow growth of a good crystal.

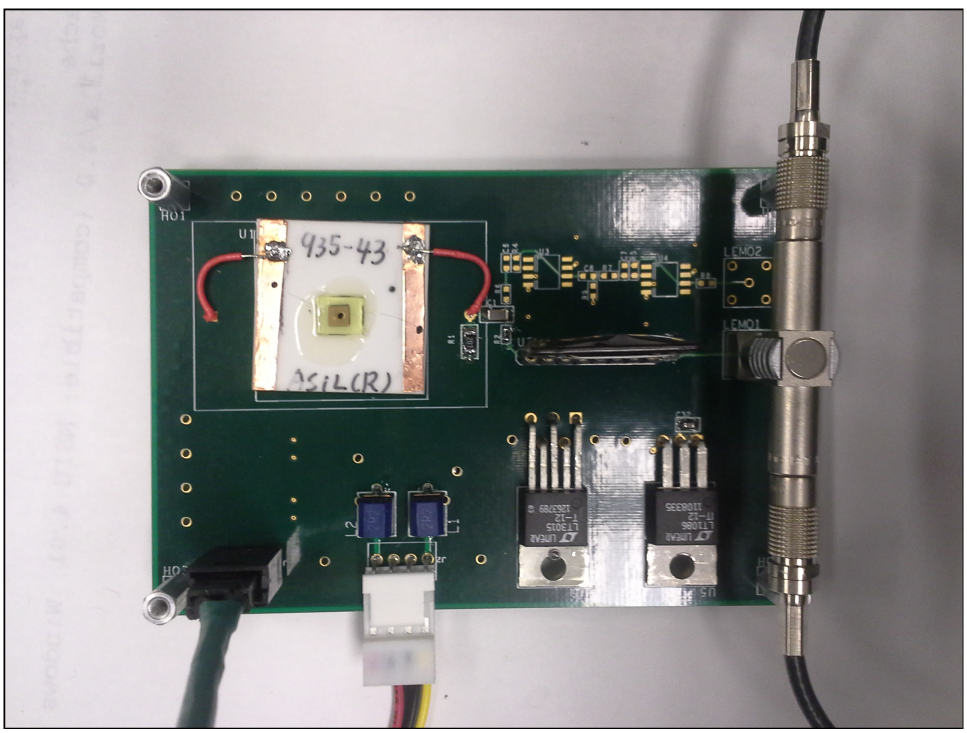

Cutting, polishing, surface treatment, electrodes

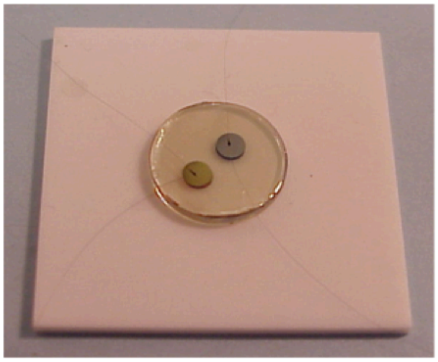

Figure 7. Photograph of a TlBr device with Au and Pd electrodes deposited on both crystal faces for comparison.

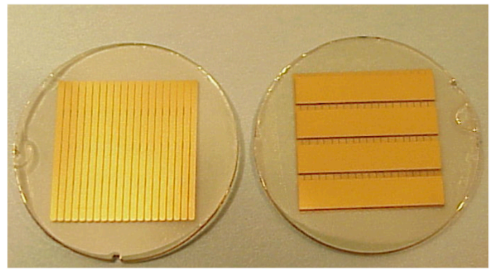

Figure 8. Photograph of two faces on 0.5 mm thick TlBr detectors with orthogonal strip design. The area covered by both sets of strips is 10x10 mm^2. One set of strips provides very high spatial resolution (0.5 mm pitch), while the coarser strips placed orthogonally to the high resolution strips provide DOI.

Timing

- Due to poor charge mobility, timing performance is the biggest drawback for useful semiconductor detectors for PET.

RMD Measurement: 0.5 mm thick detector, 350 KeV LLD, 300 V bias

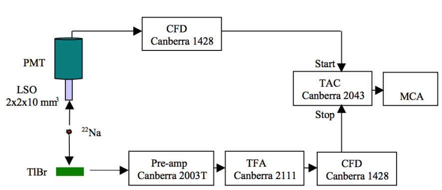

Figure 26. Schematic of the setup used to measure timing resolution of TlBr

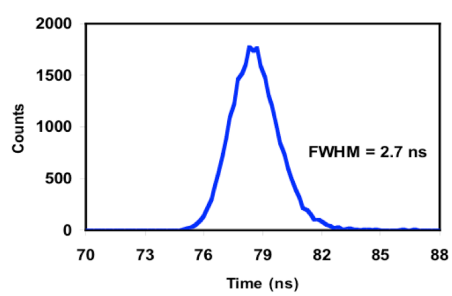

Figure 3. Timing resolution plot for a 0.5-mm thick TlBr detector in coincidence with a LSO-PMT detector and irradiated with 511 keV gamma-ray pairs.

Significant progress has been made on TlBr detector development, reflecting the improvement of material purification, crystal growth and detector fabrication techniques for TlBr over the years.

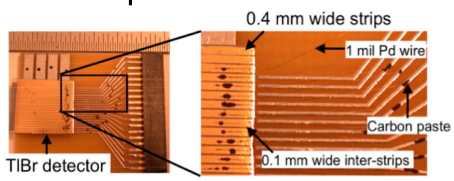

Figure 9. Photograph of a 10x10 mm^2 TlBr detector with orthogonal strip design, mounted and with electrical connections established by hand.

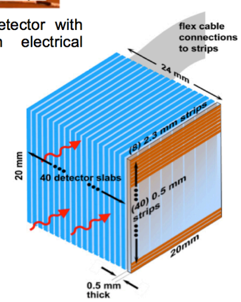

Figure 5. Schematic of TlBr PET modules with 20 x24 x20 mm^3 volume to be built by stacking 40 orthogonal strip detectors shown in Figure 4.

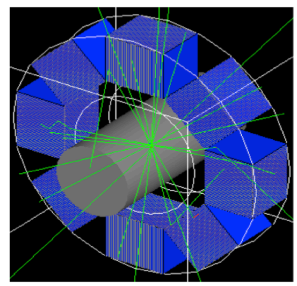

Figure 17. One-ring scanner design using blocks of TlBr detectors as developed in this project.

Large Field of View PET Scanner: EXPLORER

Why total-body PET?

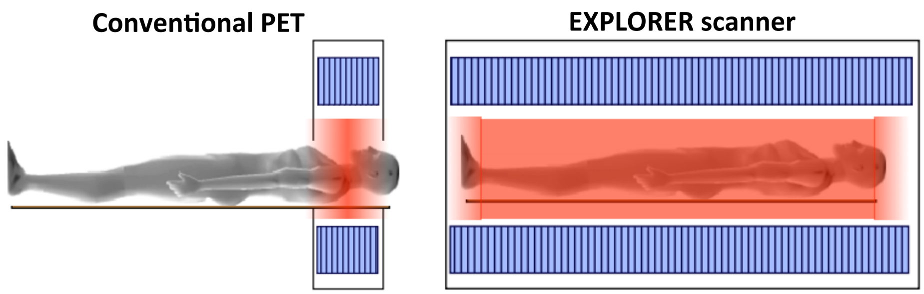

EXPLORER: 40 fold sensitivity increase for whole-body imaging

- High sensitivity data for all organs simultaneously
- Low dose imaging
- Rapid imaging
- Late stage imaging (~5 half lives)
- Improved statistical quality

Two issues: DOI and TOF

Depth-of-interaction

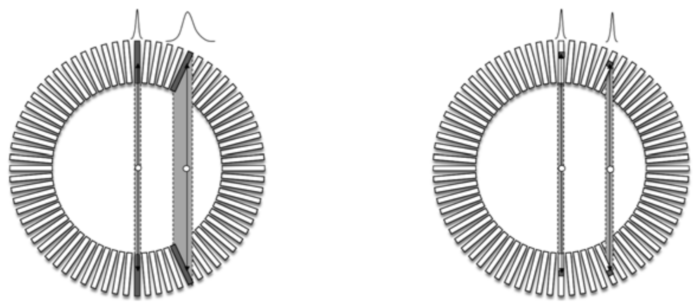

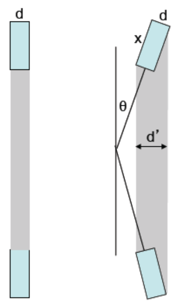

$$d' = d\cos\theta + x\sin\theta$$

$$R_{int}' \approx \frac{d'}{2} \approx \frac{d}{2} \times [\cos\theta + \frac{x}{d}\sin\theta]$$

$$R_{int}' \approx R_{int} \times [\cos\theta + \frac{x}{d}\sin\theta]$$

DOI encoding:

- Reduces effective crystal length ∝ DOI resolution.
- Improves intrinsic detector resolution for large θ

Time-of-flight

$$\Delta d = \frac{(t_1 - t_2) \times c}{2}$$

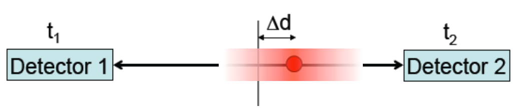

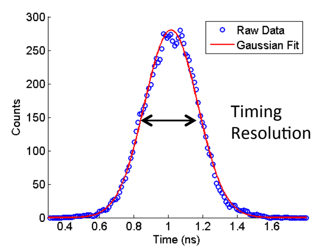

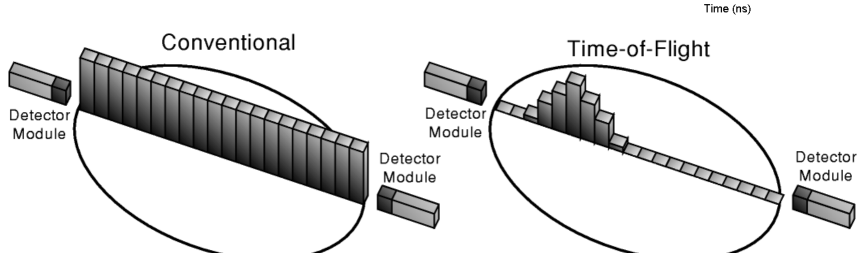

$$SNR_{TOF} = SNR\sqrt{\frac{2D}{c\Delta t}}$$

Developing TOF-DOI PET detectors needed for EXPLORER scanner

Conventional radiotracer positioning

Reduce blurring from axial DOI parallax error

Increase effective sensitivity / reduce noise with TOF

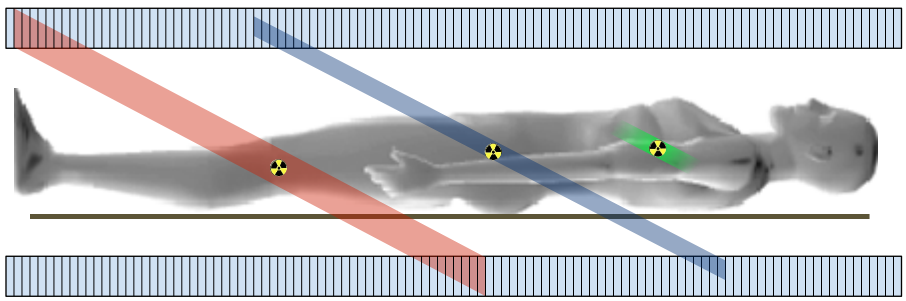

Siemens Block Detector

- 12 x 12 array of chemically etched crystals (4 x 4 x 20 mm) separated by ESR (specular/mirror-like reflector)
- Hamamatsu R9800 PMTs
- Internal light guide + 6 mm glass plate for light spreading

Detector module without metal can

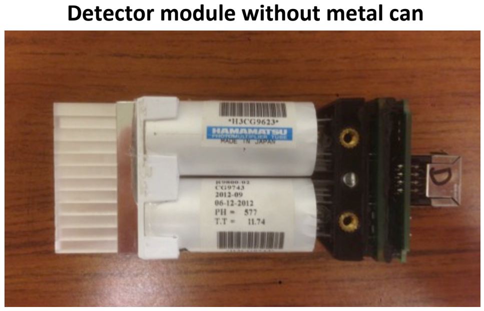

Electronics readout

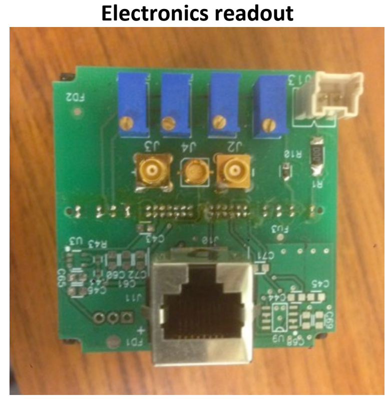

Phosphor-coated crystals for TOF - DOI

- DOI encoding with phosphor-coated crystals previously investigated (Du *et al* 2009) for small animal PET
- Phosphor layer causes depth-dependant signal shape changes

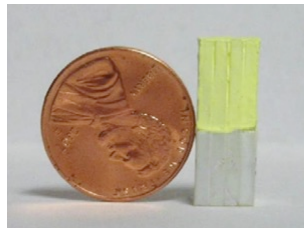

Figure from Du *et al* 2009

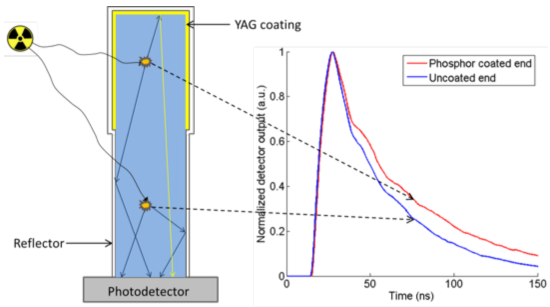

- DOI resolution = 8 mm
- Unpolished crystals → poor timing, energy
- Small crystals with PS-PMT

Preliminary investigations with single crystals

<u>Single phosphor-coated crystals directly coupled to fast PMTs</u>

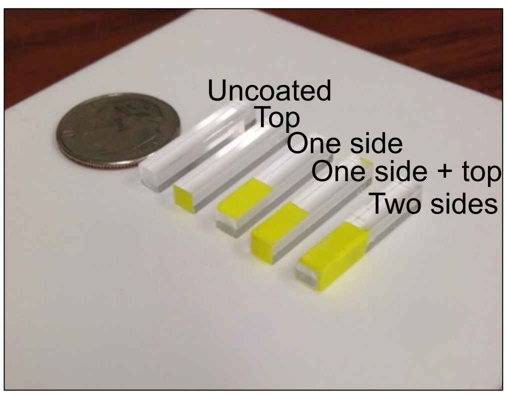

Phosphor-coated 3x3x20 mm^3 LYSO crystals.
Coating thickness ~100 µm.

Custom block detector with coated crystals

Several complete detectors with phosphor-coated crystals constructed

- Developed methods to apply phosphor coating and assemble 225 crystals
- Crystal size is 3.34 x 3.34 x 20 mm.

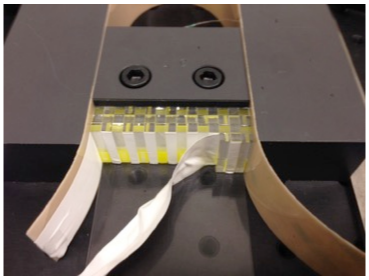

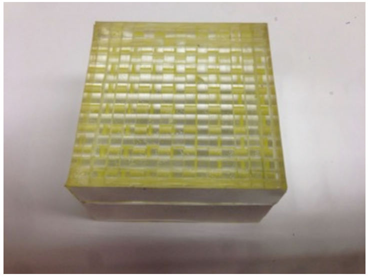

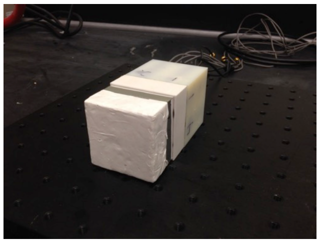

Results for central 5 x 5 crystals

Energy Resolution	13-14%
Timing Resolution	440 ps
DOI encoding	2 bins (85%)

Nuclear Imaging of Plants

SPECT: Single-Photon Emission Computed Tomography

INTRODUCTION

HEAVY METALS IN PLANTS

SPECT IMAGING

ZINC IN *ARABIDOPSIS*

ROLE OF HMA4

FUTURE DIRECTIONS

Gamma rays detected by gamma cameras

Un-collimated SPECT

Improved sensitivity
→ Improved temporal resolution
→ Less time per imaging subject
→ Less radiotracer (safety & cost)

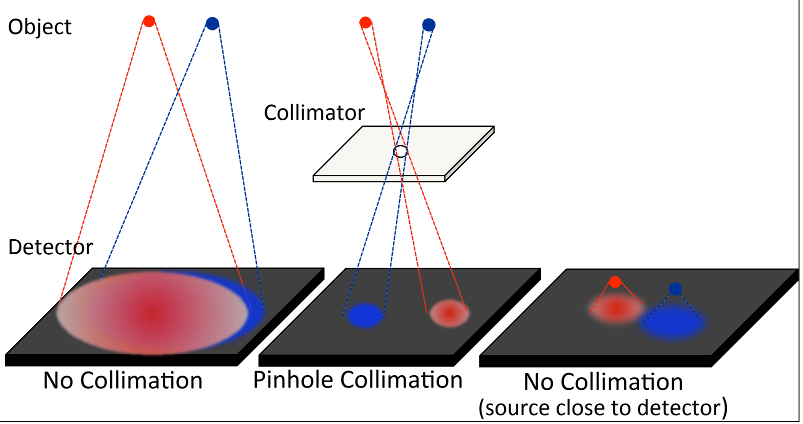

SPECT: Single-Photon Emission Computed Tomography

INTRODUCTION

HEAVY METALS IN PLANTS

SPECT IMAGING

ZINC IN *ARABIDOPSIS*

ROLE OF HMA4

FUTURE DIRECTIONS

System set-up for imaging

Two un-collimated detector heads (in red)

Flexible and compact geometry

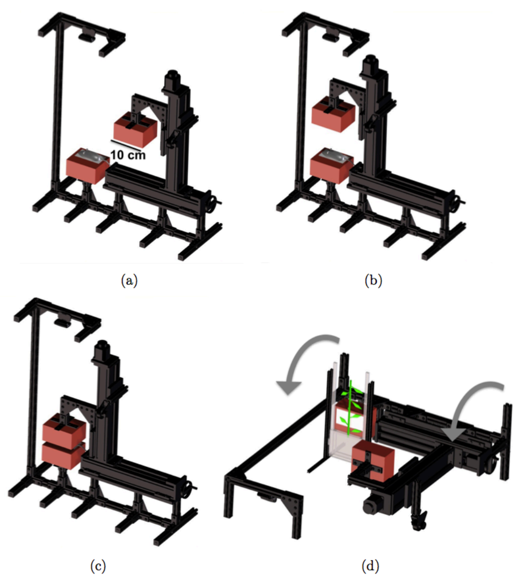

Walker KL et al., PMB, 2014

Detector Head

(Photographs)

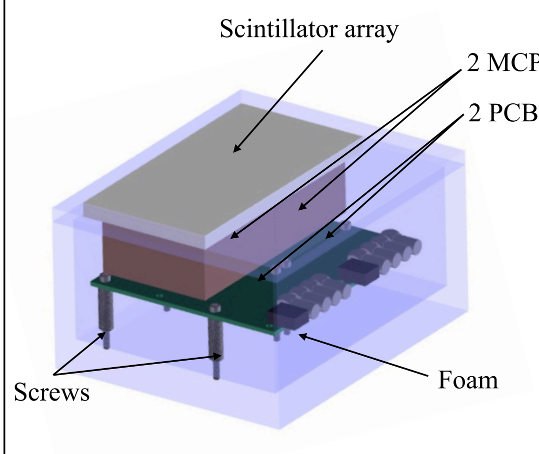

Figure from: **Walker KL**, Cherry SR, and Mitchell GS. "Detector Performance Characterization for High Sensitivity Single-Photon Imaging," *IEEE TNS*

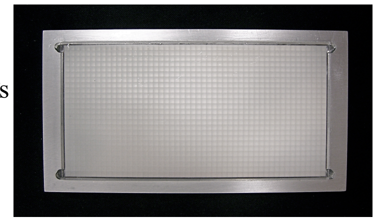

5 cm x 10 cm Scintillator

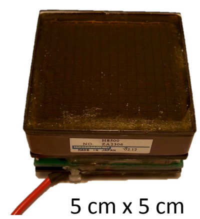

5 cm x 5 cm MCPMT

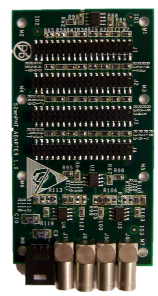

PCB

^{65}Zn dynamic scans following 1 h radioactive incubation and final nutrient water rinse. Color scale units are counts/mm²/h. [upper figure] Six frames (each 15 min long) of a scan for the *A. halleri* genotype, beginning at 0 h, 12 h, 24 h, 36 h, 48 h, and 60 h. The images show initially a signal from the roots and then a signal from the above ground biomass. [lower figure] Five frames (each 20 min long) of a scan for the *A. halleri HMA4-RNAi* genotype, beginning at 0 h, 12 h, 24 h, 36 h, and 48 h. The images show initially a signal from the roots and then dilution of that signal (back into the solution) over time; the images do not show migration of the radiotracer into the above ground biomass.

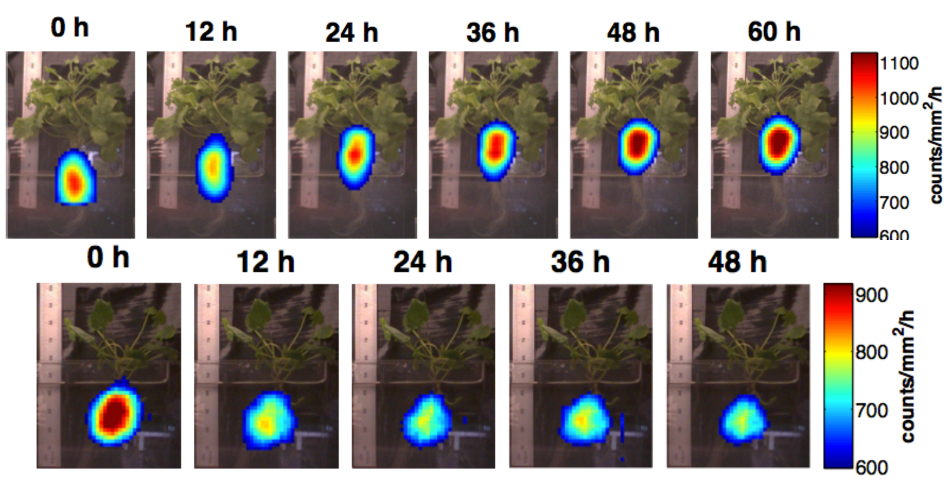

Cerenkov Imaging

Cerenkov Radiation

Optical wavelength photons emitted by fast charged particles

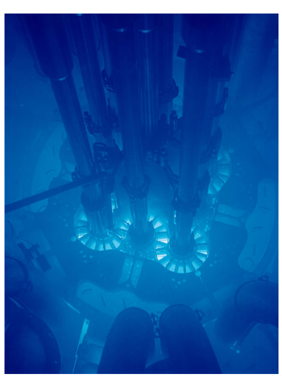

[Advanced Test Reactor, Idaho National Laboratory]

Frank-Tamm formula
(number of photons per distance traveled):

$$\frac{dN}{dx} = 2\pi\alpha\left(1 - \frac{1}{\beta^2 n^2}\right)\int_{\lambda_1}^{\lambda_2}\frac{d\lambda}{\lambda^2}$$

$\beta = v/c$ ratio of particle velocity to speed of light

n index of refraction

α fine structure constant

Threshold for Cerenkov Production

Threshold: $\beta n > 1$

For relativistic electrons/positrons, $\boldsymbol{\beta}$ is related to particle kinetic energy $\boldsymbol{E}$ by:

$$\beta = \sqrt{1 - \left(\frac{1}{\frac{E(keV)}{511} + 1}\right)^2}$$

Threshold energy in…

water	n = 1.332	E = 263 keV
tissue	n = 1.36 – 1.40	E = 219-244 keV

UCDAVIS UNIVERSITY OF CALIFORNIA cmgi

Some CLI Physics…

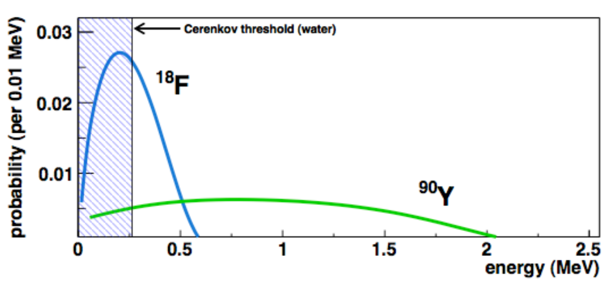

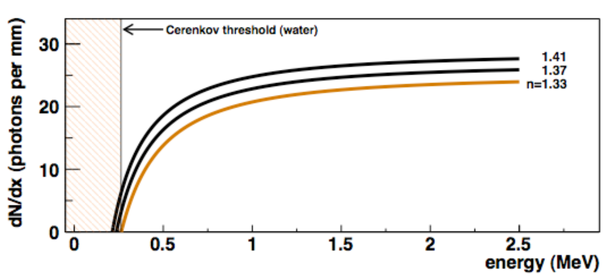

UCDAVIS UNIVERSITY OF CALIFORNIA cmgi

Monte Carlo Simulation of Spatial Distribution of Emitted Photons

(colors show the portion of each track above Cerenkov threshold)

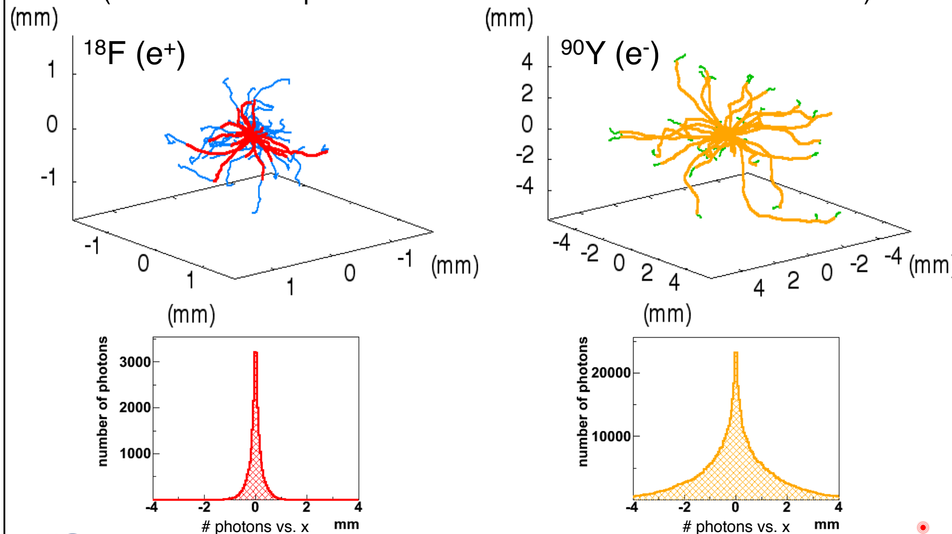

UCDAVIS UNIVERSITY OF CALIFORNIA

cmgi

Monte Carlo Simulation Results

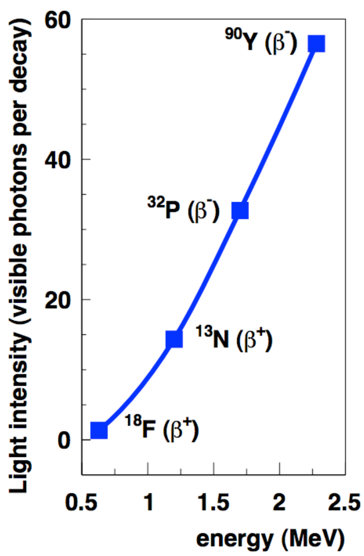

Light intensity

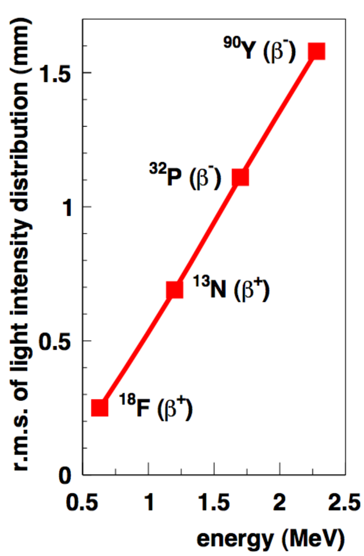

Light spatial distribution

UCDAVIS UNIVERSITY OF CALIFORNIA

cmgi

In Vivo Imaging

nu/nu mouse with U87 (glioma) cells expressing engineered antibody 2D12.5/ G54C as a reporter gene

with yttrium-(S)-2-(4-acrylamidobenzyl)- DOTA (*Y-AABD) as a reporter probe

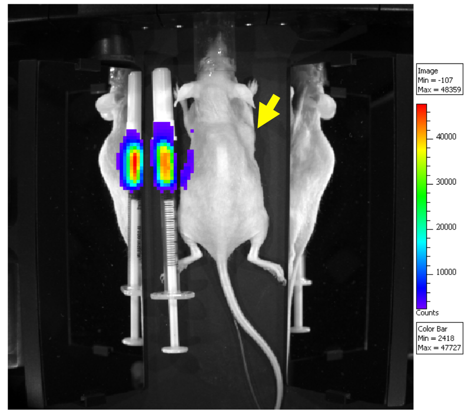

Syringe with 190 μCi ^{90}Y-AABD next to mouse (with side mirrors)

previously published reporter approach, see:
Engineered Antibody Fragments with Infinite Affinity as Reporter Genes for PET Imaging
LH Wei, et al. (2008) J Nucl Med **49** 1828–1835

UCDAVIS UNIVERSITY OF CALIFORNIA

cmg

^{90}Y Biodistribution @ 120 hrs

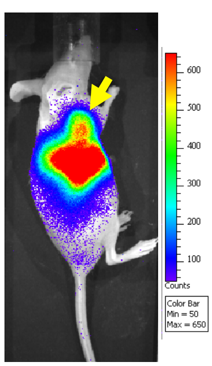

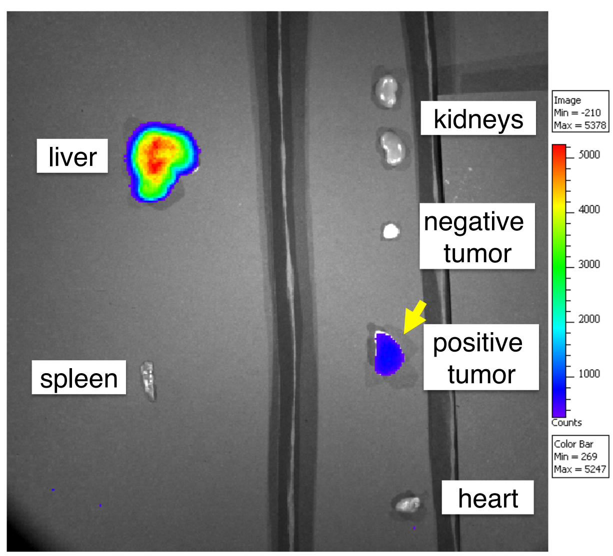

Ex vivo tumor : liver contrast = 1:5

UCDAVIS UNIVERSITY OF CALIFORNIA

cmg

Cerenkov Luminescence Imaging Example: Probe Development Screening

Aweda *et al.* Bioconjugate Chem. 2011 **22** 1479–1483
[dx.doi.org/10.1021/bc2002049]

2 similar ^{90}Y labeled molecules:
1/2/3 cohort tests ^{90}Y probe #1
A/B/C cohort test ^{90}Y probe #2

Left tumor	Right tumor
control	engineered reporter gene

~10 μCi per animal
T=48 hs post-injection

Dissected organs: tumors (arrows); heart, lungs, liver, kidneys, stomach, spleen, intestines.

Non-invasive *in vivo* imaging of beta minus emitter

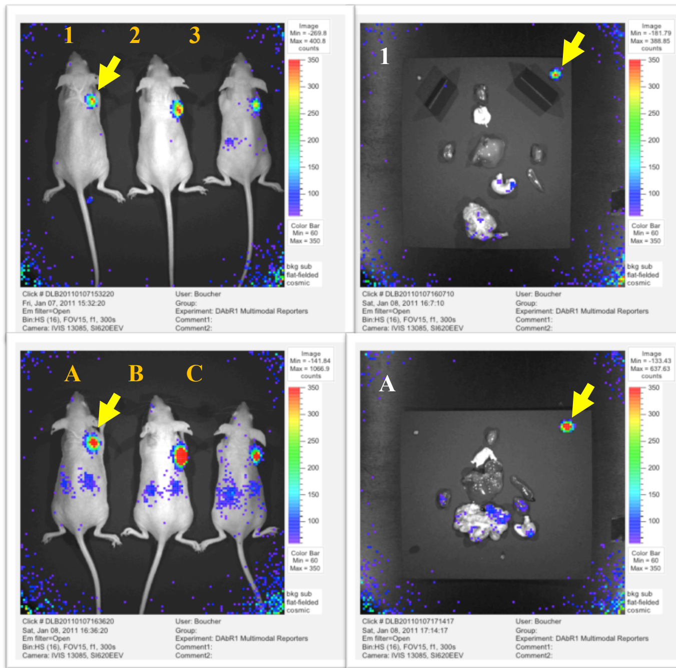

UC DAVIS
UNIVERSITY OF CALIFORNIA

cmg

Small Animal PET Imaging

Requirements

	Clinical PET	Animal PET
Sensitivity	✔	✔✔
Spatial Resolution	✔	✔✔
Energy Resolution	✔	
Timing Resolution	✔	
Count-Rate Capability	✔	
Depth-of-Interaction		✔
Detector Area	~3000-7000 cm^2	~50-500 cm^2

High Resolution Mouse Brain Scanner

16 dual-ended readout tapered detectors
FOV: axial 7 mm, transaxial 40 mm

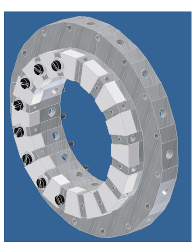

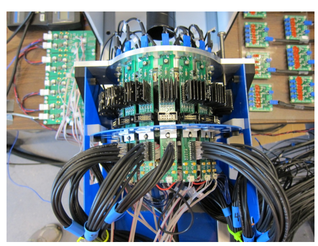

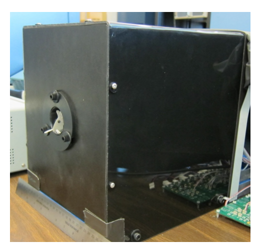

Crystal Array:
14x14 elements, LSO

Crystal size:
Front: 0.44×0.44 mm^2
Back: 0.8×0.44 mm^2

Length: 13 mm

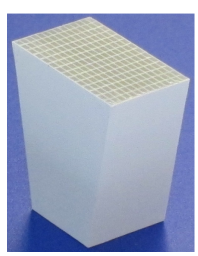

PSAPDs: Front: 10×10 mm^2
Back: 10×15 mm^2

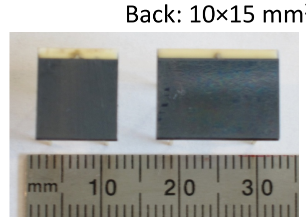

Preliminary Images

Hot spot phantom:

Capillary tube
ID: 0.75 mm
OD: 1.1 mm

Rod to rod distance:
1.5 mm

Measured reconstructed spatial resolution < 0.6 mm

Image from Inveon D-PET OSEM reconstruction

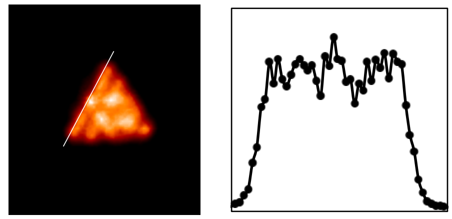

Image from prototype scanner

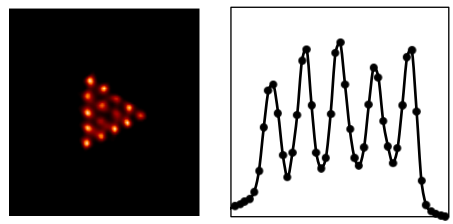

Small-animal PET is an important application area and lends itself well to early evaluation of novel radiation detector technologies for nuclear medical applications

Performance improvements are still possible and needed to address critical targets such as the mouse brain

SUMMARY

Nuclear Imaging

- Advantages:
  - High sensitivity (nM-pM)
  - Labeling of small molecules with little or no change in biological action
  - Whole body 3D volumetric imaging (tomographic)
  - Quantitative
  - Straightforward translation from mouse to man
- Disadvantages
  - Involves ionizing radiation
  - Access to radiolabeled molecules, especially for short half life radionuclides
  - Limited spatial resolution (~0.5 mm SPECT, ~ 1 mm PET)

NUCLEAR IMAGING

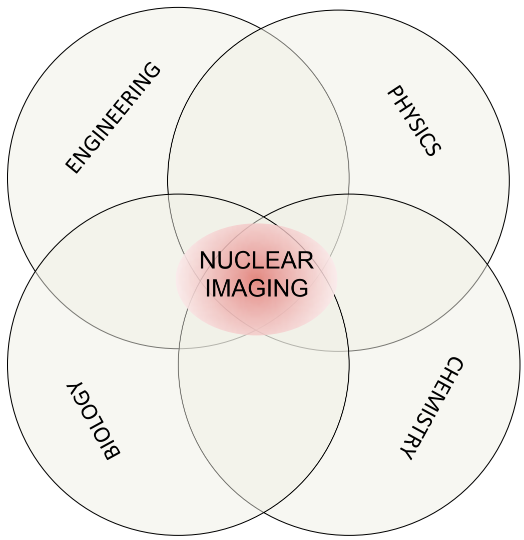

Health Care

...by the early 2020s the taxpayer will be footing the bill for half of America's health spending, which will have risen to a staggering $5 trillion, equivalent to one-fifth of the country's entire economic output.

[The Economist, Dec. 21, 2013]

- Nuclear medicine uses many techniques from nuclear physics
- Gamma-ray imaging systems (PET/SPECT) are essentially small nuclear physics experiments

Research includes:

detectors--new scintillators, photodetectors, solid-state materials

electronics & DAQ

multimodality systems

reconstruction & image processing

UCDAVIS
UNIVERSITY OF CALIFORNIA

Acknowledgements
Simon Cherry and Cherry Lab at UCD
funding: NIH and DOE